Processing and Application of Ceramics 14 [2] (2020) 141–145
https://doi.org/10.2298/PAC2002141R

Enhanced growth of $Y_3Al_5O_{12}:Ce^{3+}$ nanocrystals in mesoporous SiO_2 utilizing vacuum-assisted impregnation

Bikas Ranjan, Kenji Shinozaki, Masaru Yamashita, Tomoko Akai*

National Institute of Advanced Industrial Science and Technology (AIST), 1-8-31, Midorigaoka, Ikeda, Osaka 563-8577, Japan

Received 13 October 2019; Received in revised form 22 March 2020; Accepted 11 April 2020

Abstract

YAG:Ce nanocrystals were successfully formed within silica matrix via impregnation of a YAG:Ce precursor solution in mesoporous silica, followed by sintering. In this study, vacuum-assisted impregnation was applied to increase the size of YAG:Ce nanocrystals in a silica matrix. The size of the YAG:Ce nanocrystals stabilized in the silica matrix via impregnation under atmospheric pressure was 18 nm. By applying vacuum-assisted impregnation, the size of the nanocrystals increased to 31 nm. The photoluminescence spectra of the obtained silica-YAG:Ce composites revealed that there was an approximate three-fold increase in the intensity of emission when vacuum-assisted impregnation was applied. The internal quantum efficiency also increased from 13.6% to 32.2%.

Keywords: *nanocomposites, Ce-doped YAG, silica, optical properties*

I. Introduction

Cerium-doped yttrium aluminium garnet ($Y_3Al_5O_{12}:Ce^{3+}$ (YAG:Ce)) is an excellent phosphor employed in white LEDs as a light converter [1–3]. The synthesis of YAG:Ce nanocrystals has attracted significant interest, and numerous studies on the synthesis of nanocrystals have been conducted [4–8]. Porous materials are useful in fabricating size-controlled nanocrystals. Among the various types of porous materials, mesoporous silica is the most frequently used to support functional nanocrystals for catalysis [9,10] and phosphor [11,12] because various types of mesoporous silica with different pore properties are available.

Recently, YAG:Ce nanoparticles incorporated in mesoporous silica were synthesized by mixing a YAG:Ce solution and a silica solution with subsequent drying and sintering [13]. However, controlling the size of nanocrystals seems to be difficult because nanocrystals are likely to aggregate in a flexible silica network in the solution. To control the size of YAG:Ce nanocrystals, they should be grown in solid mesoporous silica, which works as a rigid template. However, no previous study has been reported on the incorporation of YAG:Ce nanocrystals in the rigid mesoporous silica because yttrium might easily react with silica to form yttrium silicate. To grow YAG:Ce nanocrystals in mesoporous silica, a sufficient amount of YAG:Ce precursor should be introduced in the pore before starting the sintering process. Recently, Aboulaich *et al.* [14] prepared mesoporous silica, dispersing YAG:Tb nanophosphors with high crystallinity, by *in-situ* synthesis in mesopores for the first time. They repeated impregnation of a YAG:Tb solution into mesoporous silica ten times to entirely fill the pore with YAG:Tb precursor. With subsequent sintering at 1000 °C, YAG:Tb nanocrystals were formed in mesoporous silica. However, the incorporation of YAG:Ce nanocrystals has not been reported yet probably because the control of valence state of Ce^{3+} is difficult owing to the inhomogeneity resulting from the repetitive impregnation. Moreover, repeating the impregnation ten times is tedious and time-consuming. Hence, a simpler method is required for the incorporation of the YAG:Ce precursor in the mesopores.

Herein, we propose the utilization of the vacuum-assisted impregnation, which was previously used to disperse high concentrations of metal oxide nanoparticles in mesoporous media [15,16]. Impregnation in vacuum helps in removing "air pockets" of absorbed

* Corresponding authors: tel: +81 727 51 9627,
e-mail: *t-akai@aist.go.jp*

gas in the mesopores, which hinders the introduction of the solution, leading to a homogeneous loading of a high concentration of the precursor. The structure of the obtained silica-YAG:Ce composites was examined using X-ray diffraction (XRD), scanning electron microscopy (SEM), and scanning transmission electron microscopy (STEM). The photoluminescence (PL) spectra and quantum efficiency were also investigated.

II. Experimental

2.1. Synthesis methods

In the first step, a precursor of YAG:Ce nanocrystals was prepared by dissolving $Y(NO_3)_3 \cdot 6\,H_2O$, $Al(NO_3)_3 \cdot 9\,H_2O$, and $Ce(NO_3)_3 \cdot 6\,H_2O$ in 30 ml of a 2:1 water-polyethylene glycol (PEG-200) mixture, following the procedure reported by Xiaown *et al.* [13]. Here, 4 mol% of Ce^{3+} ions with respect to Y^{3+} ions was added into the mixture. Citric acid (0.5 M) was then added to control the pH of the solution and stirred for 1 h to achieve a homogeneous mixture. As the support medium for the YAG:Ce nanocrystals, 1.5 g of mesoporous silica particles (Sigma Aldrich, Davisil grade 643, 200–425 mesh, Sigma Aldrich) was used. The mesoporous silica powder was first placed in a glass flask and kept in vacuum at 200 °C for 1 h to remove the trapped water and gas in the mesopores. After cooling to room temperature, the precursor solution was poured into the glass flask. To impregnate the mesoporous silica with a YAG:Ce precursor, the precursor solution and mesoporous silica were kept in vacuum until the release of gas bubbles from the mesoporous silica was no longer observed. The sample mixture was dried in an oil bath at 90 °C for 15 h. The sample was then sintered at 1150 °C for 3 h in air to grow the YAG:Ce nanocrystals inside mesoporous silica. To force the cerium ions to maintain a trivalent state and improve the crystallinity of YAG, the sample was further sintered in a reducing atmosphere of H_2 (5%) and Ar (95%) at 1000 °C for 7 h. To remove any surplus micro-sized YAG:Ce phosphors formed during synthesis on the surface of silica, the obtained sample was immersed in a 0.5 M NaOH solution for 24 h under vigorous stirring and then centrifuged (8000 rpm for 5 min).

To clarify the effect of vacuum impregnation, a sample without vacuum-assisted impregnation was prepared for a comparison. The sample was prepared using the same procedure described above, except that the impregnation of the precursor was undertaken in air at atmospheric pressure. The obtained sample was characterized based on a comparison with the sample prepared using vacuum-assisted impregnation.

2.2. Characterizations

The mesoporous silica particles, used as the starting material, were characterized by nitrogen adsorption method. The measurement was performed using a N_2 adsorption/desorption measurement system (Quantachrome NovaWin, NOVA instrument). The presence of a crystal phase in the obtained samples was examined through XRD, using a diffractometer (Ultima-IV, Rigaku) with Cu-$K\alpha$ radiation at 40 kV and 40 mA. For the SEM measurement, powder sample was mounted on a holder using double sided carbon-conductive tape, and coated with carbon by vacuum-evaporation. SEM images were taken on a JEOL 5600 scanning electron microscope equipped with an energy dispersive X-ray spectroscopy (EDS) system. With regard to STEM measurements, the samples were ground and suspended in an ethanol solution and loaded onto a copper mesh. The STEM/EDS measurement was performed using a Tecnai G2F20 (FEI), operating at 200 kV. The photoluminescence (PL) was measured using a photoluminescence spectrometer (F-7100, Hitachi). The sample was loaded in the stainless cell having a silica glass window. The quantum yields of both samples were measured using an integrated sphere equipped with a spectrophotometer (QE-1100, Otsuka Electronics).

III. Results and discussion

3.1. Structural characterization

Figure 1a presents the nitrogen adsorption/desorption isotherm curve of the silica powder. The isotherm exhibits typical Type IV behaviour characteristics for mesoporous materials [17]. Figure 1b presents the distribution of pore diameter analysed by the Barrett-Joyner-Halenda (BJH) method. The average pore diameter and

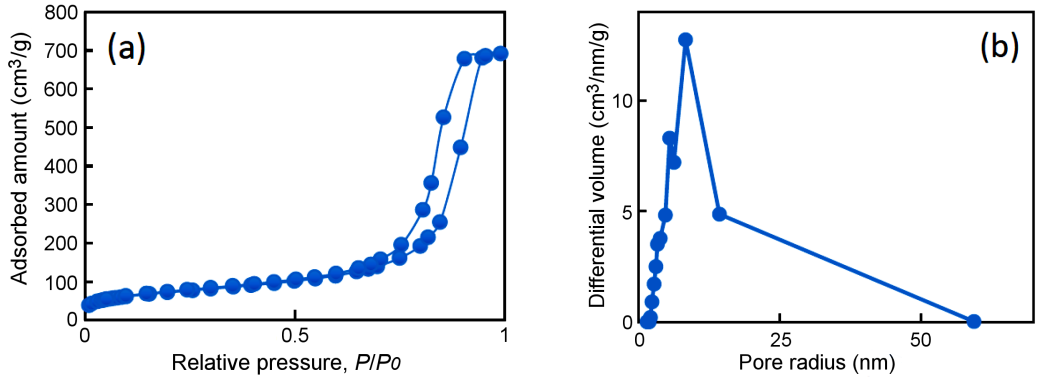

Figure 1. Adsorption/desorption isotherm (a) and pore diameter distribution (b) of porous silica used in the experiment

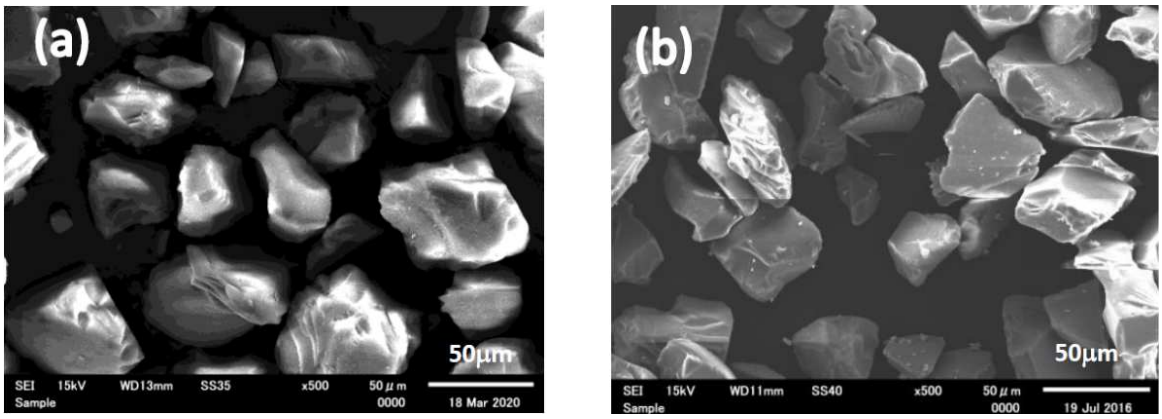

Figure 2. SEM micrograph of: a) mesoporous silica (starting material) and b) composite sample prepared via impregnation in air

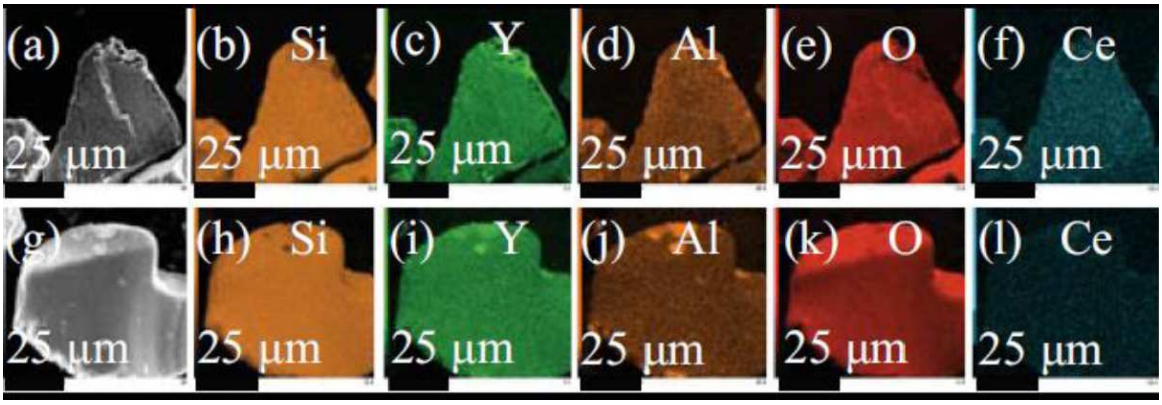

Figure 3. SEM images of the obtained silica particle prepared via impregnation in vacuum (a) and in air (g) and EDS mapping of elements of the sample prepared via impregnation in vacuum (b-f) and in air (h-l)

pore volume derived from the analysis are 17 nm and 1.07 cm^3/g, respectively.

Figures 2a and 2b present the SEM images of the starting silica particles and the finally obtained composite, respectively. In both samples the average particle size is ~50 µm, and shape of the obtained composite is similar to the original silica particles. Figures 3a and 3g show the particles obtained via impregnation in vacuum and in air, respectively. The EDS mappings of the particles prepared via impregnation in vacuum and in air are presented in Figs. 3b-f and 3h-l, respectively. The distribution of Y, Al, Si, O, and Ce is mostly uniform, meaning that majority of micro-sized YAG:Ce crystals inevitably formed on the surface of silica particles are removed with NaOH leaching.

Figure 4 shows the XRD patterns of the silica-YAG:Ce composites synthesized in vacuum and in air, along with the diffraction lines of $Y_3Al_5O_{12}$ (JCPDS 33-0040), cristobalite (JCPDS 76-0934), and quartz (JCPDS 89-8937). The diffraction lines of YAG are clear in both samples, revealing the presence of the YAG crystal phase. The average size of the YAG:Ce nanocrystals was estimated by the Scherrer's equation [18] from the width of the major line at 29.6° and 33.2°. The size of the particles in the sample prepared via impregnation in air was 18 nm, which mostly coincides with the pore size. In contrast, the size of the crystals in

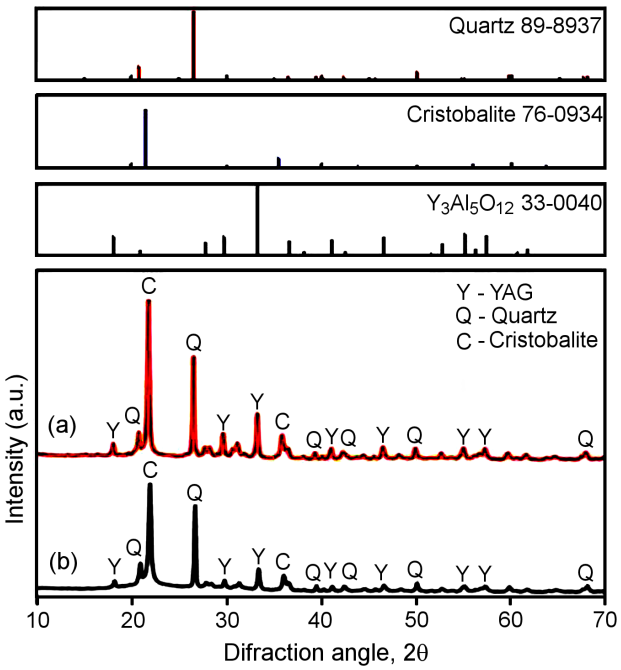

Figure 4. XRD patterns of silica-YAG:Ce composites synthesized in vacuum (red curve) and in air (black curve) together with diffraction patterns of $Y_3Al_5O_{12}$ (JCPDS 33-0040), cristobalite (JCPDS 76-0934) and quartz (JCPDS 89-8937)

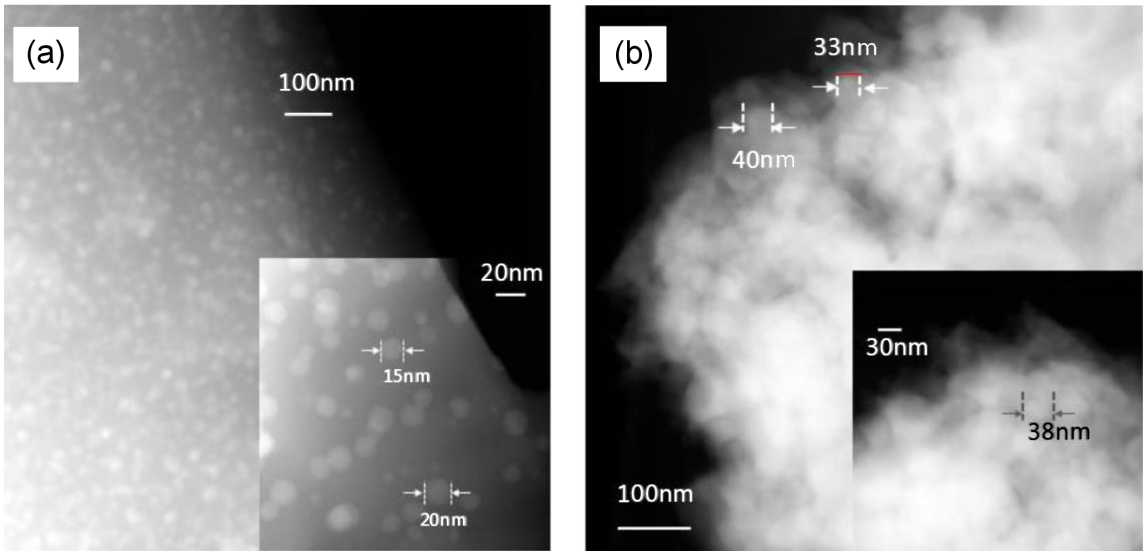

Figure 5. STEM images of the sample prepared via impregnation in: a) air and b) in vacuum

the sample prepared via vacuum-assisted impregnation was 31 nm, which is much larger than the pore diameter. Xia *et al.* [15] reported that three-dimensionally connected oxide materials are formed in mesoporous SiO_2 via vacuum-assisted impregnation with subsequent sintering at 850 °C. Different from the work of Xia *at al*, there is local structural change in the silica matrix because of the sintering at a higher temperature (1150 °C) adopted in this work; the change occurs with the collapse of the pores above 950 °C [19] and crystallization of the silica matrix observed by XRD. Hence, it is speculated that the 3D-connected YAG:Ce nano-domains are first formed in the pore, and they aggregate to form YAG:Ce particles larger than the pore size with the structural change of the silica matrix.

Figure 5 shows the STEM images of the silica-YAG:Ce composites synthesized via impregnation in vacuum and in air. Isolated particles (bright area), with typical size of ~15–20 nm, are clearly observed in the composite synthesized via impregnation in air (Fig. 5a). The average and median size of the particles are 15 nm and 16 nm, respectively. The size observed by STEM mostly agrees with that estimated by XRD. On the other hand, STEM image of the sample prepared via vacuum-assisted impregnation (Fig. 5b) confirms presence of highly concentrated particles. Accurate size of the particles cannot be determined because boundaries of the particles are not very clear, however, approximate size of the particles is frequently found between 30 and 40 nm (Fig. 5a). This observation is also consistent with XRD results. The particles are not spherical and exhibit distorted shape, strongly suggesting that particles are formed with the aggregation of the three-dimensional domains of the YAG:Ce crystals. Thus, the vacuum-assisted impregnation is proved to be effective in enhancing the growth of the particles. However, size-controlled well-isolated particles were not obtained due to the aggregation of YAG crystals formed in the pores.

3.2. *Optical properties*

Figure 6 presents the emission and excitation spectra of the samples synthesized under two different conditions. The two prime excitation peaks observed at approximately 340 and 455 nm were assigned to $4f \rightarrow 5d_2$ and $4f \rightarrow 5d_1$ transitions, respectively [5]. The PL spectra (λ_{ex} = 455 nm) of the silica-YAG:Ce composites were measured in the range of 500–700 nm, as illustrated in Fig. 6 (solid curve). The PL peak was obtained at approximately 565 nm, with a full-width broadband emission at half maxima of approximately 100 nm assigned to $5d \rightarrow 4f$ transition. The intensity of emission for the sample impregnated in vacuum was almost three times higher (red curve) than that for the sample impregnated in air (black curve).

The colour coordinates of the Commission Internationale de l'Eclairage (CIE) for both samples are (0.44, 0.53), and a yellow light was observed. For the sample

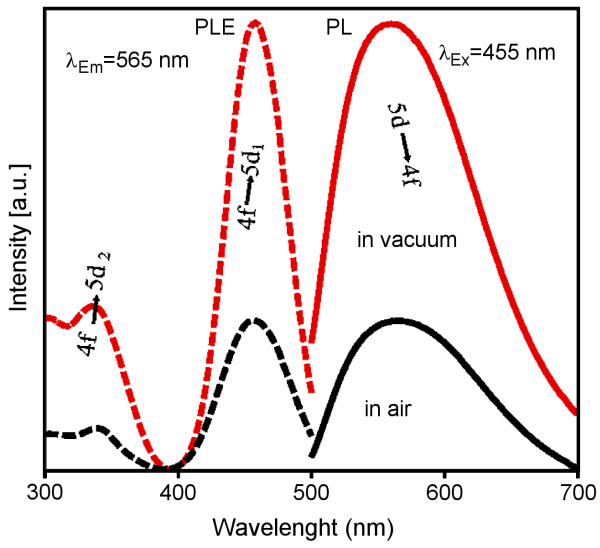

Figure 6. PL spectra of silica-YAG:Ce composites impregnated in vacuum (red curve) and in air (black curve)

impregnated in air, the internal PL quantum yield (IQY), external quantum yield, and the absorption obtained were 13.6%, 5.6%, and 41.1%, respectively. In contrast, these values respectively increased up to 32.2%, 23.5%, and 66.8% in the sample impregnated in vacuum. Typically, nano-sized YAG:Ce crystals obtained through the solution process lie between ~18% and 38% [7,20]. Hence, IQY in the present work, which is not very high, is attributed to the small size of crystals.

IV. Conclusions

YAG:Ce nanocrystals were successfully grown inside a silica matrix by immersing the precursor solution into mesoporous silica, followed by sintering at 1150 °C. The effect of evacuation during immersion was investigated. It was found that the vacuum-assisted impregnation significantly enhanced the growth of YAG:Ce nanoparticles, i.e. the size of the YAG:Ce particles increased from 18 to 31 nm. The IQY of the obtained sample was enhanced from 13.6% to 32.2%. Hence, it can be concluded that the vacuum-assisted impregnation was effective in enhancing the growth of YAG:Ce nanoparticles in mesoporous silica.

References

1. Y.H. Kim, N.S.M. Viswanath, S. Unithrattil, H.J. Kim, W. Bin Im, "Review-phosphor plates for high-power LED applications: Challenges and opportunities toward perfect lighting", *ECS J. Solid State Sci. Technol.*, **7** (2018) R3134–R3147.
2. G. Li, Y. Tian, Y. Zhao, J. Lin, "Recent progress in luminescence tuning of Ce^{3+} and Eu^{2+}-activated phosphors for pc-WLEDs", *Chem. Soc. Rev.*, **44** (2015) 8688–8713.
3. Z. Xia, A. Meijerink, "Ce^{3+}-doped garnet phosphors: Composition modification, luminescence properties and applications", *Chem. Soc. Rev.*, **46** (2017) 275–299.
4. Z. Wu, X. Zhang, W. He, Y. Du, N. Jia, G. Xu, "Preparation of YAG:Ce spheroidal phase-pure particles by solvothermal method and their photoluminescence", *J. Alloys Compd.*, **468** (2009) 571–574.
5. C.H. Lu, H.C. Hong, R. Jagannathan, "Sol-gel synthesis and photoluminescent properties of cerium-ion doped yttrium aluminium garnet powders", *J. Mater. Chem.*, **12** (2002) 2525–2530.
6. R. Kasuya, T. Isobe, H. Kuma, "Glycothermal synthesis and photoluminescence of YAG:Ce^{3+} nanophosphors", *J. Alloys Compd.*, **408-412** (2006) 820–823.
7. T. Isobe, "Glycothermally synthesized YAG:Ce^{3+} nanophosphors for blue LEDs", *ECS J. Solid State Sci. Technol.*, **2** (2013) 3012–3017.
8. X. He, X. Liu, R. Li, B. Yang, K. Yu, M. Zeng, R. Yu, "Effects of local structure of Ce^{3+} ions on luminescent properties of $Y_3Al_5O_{12}$:Ce nanoparticles", *Sci. Rep.*, **6** (2016) 1–11.
9. A.E. Fernandes, A.M. Jonas, "Design and engineering of multifunctional silica-supported cooperative catalysts", *Catal. Today*, **334** (2019) 173–186.
10. C. Soumini, S. Sugunan, S. Haridas, "Copper oxide modified SBA-15 for the selective vapour phase dehydrogenation of cyclohexanol to cyclohexanone", *J. Porous Mater.*, **26** (2019) 631–640.
11. N. Tripathi, M. Yamashita, T. Akai, "Synthesis and improved emission characteristics of BCNO@silica composites", *J. Mater. Chem. C*, **2** (2014) 622–625.
12. Y. Li, B. Yan, "Functionalized mesoporous SBA-15 with CeF_3:Eu^{3+} nanoparticle by three different methods: Synthesis, characterization, and photoluminescence", *Nanoscale Res. Lett.*, **5** (2010) 701–708.
13. A. Revaux, G. Dantelle, N. George, R. Seshadri, T. Gacoin, J.P. Boilot, "A protected annealing strategy to enhanced light emission and photostability of YAG:Ce nanoparticle-based films", *Nanoscale*, **3** (2011) 2015–2022.
14. A. Aboulaich, N. Caperaa, H. El Hamzaoui, B. Capoen, A. Potdevin, M. Bouazaoui, G. Chadeyron, R. Mahiou, "In situ synthesis of a highly crystalline Tb-doped YAG nanophosphor using the mesopores of silica monoliths as a template", *J. Mater. Chem. C*, **3** (2015) 5041–5049.
15. Y. Xia, Y. Zhao, Y. Li, F. Hu, L. Zhang, W. Chen, "Vacuum-assisted hard-templating impregnation fabrication of three-dimensional ordered mesoporous samarium oxide", *J. Porous Mater.*, **23** (2016) 1591–1595.
16. Y. Liu, Q. Zhao, X. Li, Y. Shi, T. Li, "Vacuum-assisted impregnation derived α-Bi_2O_3-TiO_2 nanotube arrays with enhanced photoelectrochemical activity", *Mater. Lett.*, **158** (2015) 104–107
17. K.S.W. Sing, D.H. Everett, R.A.W. Haul, L. Moscou, R.A. Pierotti, J. Rouquerol, T. Siemieniewska, "Reporting physisorption data for gas/solid systems with special reference to the determination of surface area and porosity", *Pure Appl. Chem.*, **57** (1985) 603–619.
18. A.L. Patterson, "The diffraction of X-rays by small crystalline particles", *Phys. Rev.*, **56** (1939) 972–977.
19. T. Akai, M. Murakami, M. Yamashita, T. Okajima, N. Umesaki, "Sintering process of Eu doped luminescent glass prepared from porous glass", *IOP Conf. Series: Mater. Sci. Eng.*, **18** (2011) 112001.
20. R. Kasuya, T. Isobe, H. Kuma, J. Katano, "Photoluminescence enhancement of PEG-modified YAG:Ce^{3+} nanocrystal phosphor prepared by glycothermal method", *Phys. Chem. B*, **109** (2005) 22126–22130.